Growth of NbO$_2$ by Molecular-Beam Epitaxy and Characterization of its Metal-Insulator Transition

Lindsey E. Noskin[1], Ariel Seidner H.[1], and Darrell G. Schlom[1,2]
[1] Department of Materials Science and Engineering, Cornell University, Ithaca, NY 14853, U.S.A.
[2] Kavli Institute at Cornell for Nanoscale Science, Ithaca, NY 14853, U.S.A.

ABSTRACT

Thin films of NbO$_2$ are synthesized by oxide molecular-beam epitaxy on (001) MgF$_2$ substrates, which are isostructural (rutile structure) with NbO$_2$. Two growth parameters are systematically varied in order to identify appropriate growth conditions: growth temperature and the partial pressure of O$_2$ during film growth. θ-2θ X-ray diffraction measurements identify two dominant phases in this system at background oxygen pressures in the $(0.2–6) \times 10^{-7}$ Torr range: rutile NbO$_2$ is favored at higher growth temperature, while Nb$_2$O$_5$ forms at lower growth temperature. Electrical resistivity measurements were made between 350 K and 675 K on three epitaxial NbO$_2$ films in a nitrogen ambient. These measurements show that NbO$_2$ films grown in higher partial pressures of molecular oxygen have larger temperature-dependent changes in electrical resistivity and higher resistivity at room temperature.
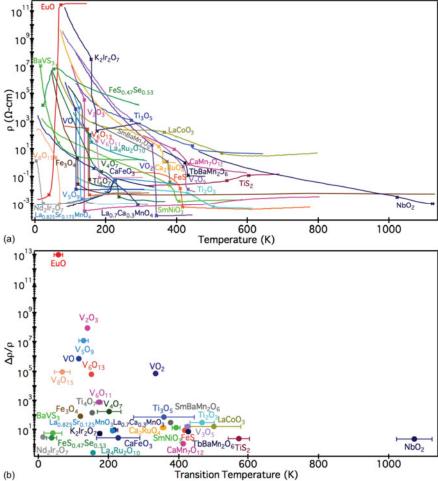
INTRODUCTION

Though rare, metal-to-insulator transitions (MITs) occur in some materials and can be triggered by an external stimulus, e.g., a change in temperature, pressure, or the application of light [1]. Figure 1(a) shows the temperature-dependent metal-insulator transitions of single-crystal MIT materials gleaned from the literature [2-27]. The resistivity data shown was selected from the literature as exemplary due to its large and sudden change in resistivity. The data in Fig. 1 is limited to materials where the MIT is an intrinsic property of the material, i.e., not due to the formation of filaments, or chemical reactions, or recrystallization. For this reason, the data is restricted to high-quality single crystals, where intrinsic behavior is most likely to be exhibited.

Changes in electrical resistivities due to MITs can be several orders of magnitude in size and very sharp as quantified in Fig. 1(b), where the change in the electrical resistivity and the temperature of the transition are plotted for each material. The transition region (between the start and end of the MIT, each denoted by an "x") was calculated by finding the second derivative of a 5-point moving smooth utilizing a cubic least-squares best-fit function to the data [28, 29]. The criteria for the points marked by "x" is that $\left| \frac{\partial^2 (\log \rho)}{\partial T^2} \right| < 1 \times 10^{-3}$, except for CaFeO$_3$, V$_8O_{15}$, BaVS$_3$, FeS$_{0.47}Se_{0.53}$, TiS$_2$, NbO$_2$, V$_4O_7$ and LaCoO$_3$, where the "x" marks for all but NbO$_2$ were specified manually due to the broad transitions involved. For NbO$_2$, the "x" marks were specified based on previous research using x-ray diffraction to detect the presence or absence of dimerization, which is the mechanism of the MIT of NbO$_2$ [30].

Materials with temperature-dependent MITs have gained attention for potential use in conjunction with metal-oxide-semiconductor field-effect transistors (MOSFETs) to reduce the sub-threshold slope of MOSFETs to beat the 60 mV/decade Boltzmann limit [31]. For VO$_2$ thin films, the MIT can be triggered electrically by applying a voltage to the films at a temperature below the MIT [32]. Previous research showing the feasibility of integrating an MIT material in series with the source of a FET device utilized VO$_2$ as the MIT material [31]. To achieve practical MOSFET operation temperatures, however, MIT materials with transition temperatures below 400 K are unsuitable, as FET devices in typical real-world applications need to perform

3031

reliably at temperatures as high as approximately 400 K [33]. The necessity for the transition to take place at temperatures above 400 K rules out most MIT materials, including VO_2.

One of the few materials with an MIT occurring above 400 K (called high-temperature MIT materials) and a substantial change in the magnitude of the electrical resistivity is NbO_2, which is shown in Fig. 1(a) [4]. As temperature increases from 400 K to 1100 K, the electrical

Fig. 1: (a) Electrical resistivity versus temperature of common MIT materials. X-symbols denote the start and end to the MIT of each given material. **(b)** Relative change in electrical resistivity versus temperature of common MIT materials. Data for the resistivity versus temperature of each material was extracted from separate publications [2-27] to make these comprehensive plots.

3032

resistivity of NbO_2 changes by more than three orders of magnitude. On account of its large electrical resistivity change at a relatively high temperature, NbO_2 is a promising material for thin film technological applications utilizing an MIT. Electrical resistivity measurements of NbO_2 thin films at high temperature have not, however, been reported. In this paper we describe the synthesis of epitaxial thin films of NbO_2 on MgF_2 by oxide molecular beam epitaxy (MBE) and high-temperature electrical resistivity measurements of these films.

EXPERIMENT

Synthesis of NbO_2 by MBE

All NbO_2 films in this paper were grown by MBE in a Veeco Gen10 chamber. X-ray diffraction spectra were measured by a Rigaku Smartlab system using Cu $K_{\alpha 1}$ radiation, a 220 Ge two-bounce incident-beam monochromator and a 220 Ge two-bounce diffraction analyzer crystal. Epitaxial thin films of NbO_2 were deposited on MgF_2 (001). MgF_2 was the selected substrate due to its availability, rutile structure, and relatively small lattice mismatch with the desired NbO_2 film. The lattice parameters of NbO_2, MgF_2, and other important materials with the rutile-structure are shown in Fig. 2(a). Epitaxial NbO_2 (001) grown on MgF_2 (001) is illustrated in Fig. 2(b). A lattice mismatch of 4.1 % was calculated with from the lattice constants [34, 35].

Single crystal, epitaxial thin films of NbO_2 were synthesized by MBE on MgF_2. To form an epitaxial film of the desired phase (NbO_2), growth parameters were varied. All niobium oxide films were grown individually with a constant deposition flux of niobium (1.7×10^{13} atoms/cm^2) at temperatures ranging from 600 °C to 800 °C in background partial pressures of O_2 ranging from 2×10^{-8} to 6×10^{-7} Torr. All films were grown to a thicknesses between 85 and 95 nm. All films were monitored during growth by reflection high-energy electron diffraction.
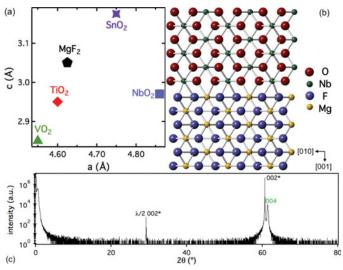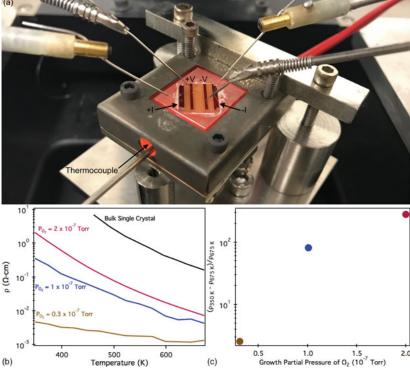

Fig. 2: (a) Plot of the lattice parameters, a and c, of common crystals with the rutile structure including NbO_2. **(b)** Schematic cross-section of the epitaxial configuration of a NbO_2 (001) film on a MgF_2 (001) substrate, where niobium atoms are represented by relatively small dark green atoms, oxygen by large dark red atoms, magnesium by small light yellow atoms, and fluoride by larger light purple atoms. **(c)** θ-2θ x-ray diffraction spectrum of an NbO_2 (001) film on a MgF_2 (001) substrate with " * " denoting peaks arising from the substrate.

3033

Single-phase thin films of rutile NbO_2 were achieved at growth temperatures between 660 °C to 770 °C and partial pressure of O_2 from 3×10^{-8} to 2×10^{-7} Torr. Undesired phases, NbO and Nb_2O_5, grew when the ambient temperature was above 770 ºC or below 660 ºC, respectively.

Fig. 3: (a) A photo of the 4-point electrical resistivity apparatus taken during the measurement of the resistivity of a NbO_2 film at 1200 K. The various parts of the setup are labeled, including the evaporated Pt/Cr contacts deposited on top of the film. **(b)** High temperature electrical resistivity measurements of three NbO_2 thin films grown by MBE at the noted partial pressures of molecular oxygen together with the resistivity data from a bulk single crystal of NbO_2 [4]. **(c)** Temperature dependent relative change in electrical resistivity of NbO_2 thin films versus the background partial pressure of molecular oxygen in which they were grown.

X-ray diffraction θ-2θ scans were used to identify the crystal structure of each niobium oxide film. The diffraction patterns obtained matched the anticipated patterns for the phase-pure crystal structure of NbO_2 (001) as shown in Fig. 2(c).

High-Temperature Electrical Resistivity Measurements

A high-temperature 4-point electrical resistivity measurement apparatus was developed to measure the MIT of NbO_2 thin films from 298 to 1200 K. This apparatus is shown in Fig. 3(a).

The setup includes a Keithley SourceMeter 2450 used as a current source, a Hewlett Packard 34401A Multimeter as a voltage meter, and a 950S Eurotherm temperature controller. Figure 3(a) shows where the appropriate probe tips were placed on the sample for measurement. A 10 nm thick adhesion layer of chromium followed by a 200 nm thick contact layer of platinum were evaporated onto the film surface to provide contact to the sample. Samples were attached to the heater surface using Ted Pella Leitsilber 200 conductive 45% silver paint. Despite the capability of heating samples to 1200 K, films heated hotter than 500 K in air were found to oxidize and become Nb_2O_5. This oxidation occurs because Nb_2O_5 is the thermodynamically stable phase in 1 atm of air. Previous research on NbO_2 at high temperature did not encounter this as those measurements were taken in either a vacuum or hydrogen ambient [4]. To prolong film oxidation, the electrical resistivity measurements presented here were taken by surrounding the measurement apparatus with a large plastic bag full of flowing nitrogen gas.

The electrical resistivity was measured on three epitaxial NbO_2 films in a nitrogen ambient. Resistivity measurements were taken every 25 K while heating. The results of these measurements, alongside published single crystal data [4], are shown in Fig. 3(b), where partial pressures of molecular oxygen during growth are noted. A trend is evident in Fig. 3(c) between the relative change in electrical resistivity and the background partial pressure of molecular oxygen during growth. As the partial pressure of molecular oxygen during growth increases, the relative change in electrical resistivity also increases. This is thought to be a result of oxygen vacancies doping the films with excess electrons, thus reducing the room temperature electrical resistivity as well as the magnitude of the change in electrical resistivity.

CONCLUSIONS

Epitaxial thin films of NbO_2 were synthesized by MBE on (001) MgF_2 substrates in background oxygen pressures in the $(0.2–6)\times10^{-7}$ Torr range at growth temperatures above 660 °C, as identified by θ-2θ x-ray diffraction measurements. Electrical resistivity measurements taken above 350 K and 675 K on three NbO_2 films in nitrogen gas show that NbO_2 films grown in higher partial pressures of molecular oxygen have larger temperature-dependent changes in electrical resistivity and higher resistivity at room temperature.

ACKNOWLEDGEMENTS

REFERENCES

[1] M. Imada, A. Fujimori, and Y. Tokura, "Metal-Insulator Transitions," Rev. Mod. Phys. **70**, 1039 (1998).
[2] A. Huon, A Lang, D. Saldana-Greco, J Lim, E. Moon, A. Rappe, M. Taheri, and S. May, "Electronic Transition Above Room Temperature in $CaMn_7O_{12}$ Films," Appl. Phys. Lett. **107**, 142901 (2015).
[3] A. Urushibara, Y. Moritomo, T. Arima, A. Asamitsu, G. Kido, and Y. Tokura, "Insulator-Metal Transition and Giant Magnetoresistance in $La_{1-x}Sr_xMnO_3$," Phys. Rev. B **51**, 103-109 (1995).
[4] G. Belanger, J. Destry and G. Perluzzo, "Electron-Transport in Single-Crystals of Niobium Dioxide," Can. J. Phys. **52**, 2272 (1974).
[5] G. Cao, S. McCall, M. Shepard, J. Crow, and R. Guertin, "Magnetic and Transport Properties of Single-Crystal Ca_2RuO_4: Relationship to Superconducting Sr_2RuO_4," Phys. Rev. B **56**, R2916-R2919 (1997).
[6] H. Okinaka, K. Kosuge, S. Kachi, K. Nagasawa, Y. Bando and T. Takada, "Electrical Properties of V_8O_{15} Single Crystal," Phys. Lett. **33A**, 370-371 (1970).
[7] J. Feinleib and W. Paul, "Semiconductor-To-Metal Transition in V_2O_3," Phys. Rev. **155**, 842-855 (1967).
[8] J. Fujioka, S. Ishiwata, Y. Kaneko, Y. Taguchi and Y. Tokura, "Variation of Charge Dynamics Upon the Helimagnetic and Metal-Insulator Transitions for Perovskite $AFeO_3$ (A = Sr and Ca)," Phys. Rev. B **85**,

3035

155141-2 (2012).

[9] J. Pérez-Cacho, J. Blasco, J. García, M. Castro and J. Stankiewicz, "Study of the Phase Transitions in SmNiO₃," J. Phys. Condens. Matter **11**, 405-415 (1999).

[10] K. Bartwal and O. Srivastava, "Studies of Metal-Insulator-Transition in TiS$_x$Se$_{2-x}$ Single-Crystals," Phase Trans. **20**, 73-81 (1990).

[11] L. A. Ladd and W. Paul, "Optical and Transport Properties of High Quality Crystals of V₂O₄ Near Metallic Transition Temperature," Solid State Commun. **7**, 425-428 (1969).

[12] M. Isobe, S. Koishi, N. Kouno, J. Yamura, T. Yamauchi, H. Hirotada, T. Yagi, and Y. Ueda, "Observation of Metal–Insulator Transition in Hollandite Vanadate, K₂V₈O₁₆," J. Phys. Soc. Jpn. **75**, 073801-2 (2006).

[13] M. Matuura, H. Hiraka, K. Yamada, and Y. Endoh, "Magnetic Phase Diagram and Metal-Insulator Transition of NiS$_{2-x}$Se$_x$," J. Phys. Soc. Jpn. **69**, 1503-1508 (2000).

[14] M. Murakami, "Anisotropy of Electrical Conduction in Iron Sulfide Single Crystal," J. Phys. Soc. **16**, 187-195 (1961).

[15] M. Onoda, "Phase Transitions of Ti₃O₅," J. Solid State Chem. **136**, 67-73 (1998).

[16] O. Massenet, J. Since, J. Mercier, M. Avignon, R. Buder, and V. Nguyen, "Magnetic and Electric Properties of BaVS₃ and BaV$_x$Ti$_{1-x}$S₃," J. Phys. Chem. Solids **40**, 573-577 (1979).

[17] P.A. Miles, W.B. Westphal and A. von Hippel, "Dielectric Spectroscopy of FerroMagnetic Semiconductors," Rev. Mod. Phys. **29**, 279-307 (1957).

[18] P. Khalifah, R. Osborn, Q. Huang, H. Zandbergen, R. Jin, Y. Liu, D. Mandrus, and R. Cava, "Orbital Ordering Transition in La₄Ru₂O₁₀," Science **297**, 2237 (2002).

[19] S.H. Shin, G.V. Chandrashekhar, R.E. Loehman and J.M. Honig, "Thermoelectric Effects in Pure and V-Doped Ti₂O₃ Single-Crystals," Phys. Rev. B **8**, 1364-1372 (1973).

[20] V.N. Andreev and V.A. Klimov, "Specific Features of the Electrical Conductivity of V₄O₇ Single-Crystals," Phys. Solid State **51**, 2235-2240 (2009).

[21] V.N. Andreev and V.A. Klimov, "Specific Features of Electrical Conductivity of V₃O₅ Single-Crystals," Phys. Solid State **53**, 2424-2430 (2011).

[22] S. Kachi, K. Kosuge and H. Okinaka, "Metal-Insulator Transition in V$_n$O$_{2n-1}$," J. Solid State Chem. **6**, 258-270 (1973).

[23] S. Lakkis, C. Schlenker, B.K. Chakraverty and R. Buder, "Metal-Insulator Transitions in Ti₄O₇ Single-Crystals Crystal Characterization, Specific-Heat, and Electron-Paramagnetic Resonance," Phys. Rev. B **14**, 1429-1440 (1976).

[24] S. Yamaguchi, Y. Okimoto, H. Taniguchi and Y. Tokura, "Spin-State Transition and High-Spin Polarons in LaCoO₃," Phys. Rev. B **53**, R2926-R2929 (1996).

[25] S. Yonezawa, Y. Muraoka, Y. Ueda and Z. Hiroi, "Epitaxially Strain Effects on the Metal-Insulator Transition in V₂O₃ Thin Films," Solid State Commun. **129**, 245-248 (2004).

[26] T. Penney, M.W. Shafer and J.B. Torrance, "Insulator-Metal Transition and Long-Range Magnetic Order in EuO," Phys. Rev. B **5**, 3669-3674 (1972).

[27] Z. Tian, Y. Kohama, T. Tomita, H. Ishizuka, T. Hsieh, J. Ishikawa, K. Kindo, L. Balents and S. Nakatsuji, "Field-Induced Quantum Metal–Insulator Transition in the Pyrochlore Iridate Nd₂Ir₂O₇," Nat. Phys. **12**, (2016).

[28] J. Tashman, J. Lee, H. Paik, J. Moyer, R. Misra, J. Mundy, T. Spila, T. Merz, J. Schubert, D. Muller, P. Schiffer and D. Schlom, "Epitaxial Growth of VO₂ by Periodic Annealing," Appl. Phys. Lett. **104**, 063104 (2014).

[29] A. Savitzky and M. Golay, "Smoothing and Differentiation of Data by Simplified Least Squares Procedures," Anal. Chem. **36**, 1627 (1964).

[30] T. Sakata, K. Sakata, and I. Nishida, "Study of Phase Transition in NbO₂," Phys. Stat. Sol. **20**, K155 (1967).

[31] N. Shukla, A.V. Thathachary, A. Agrawal, H. Paik, A. Aziz, D.G. Schlom, S.K. Gupta, R. Engel-Herbert, S. Datta, "A Steep-Slope Transistor Based on Abrupt Electronic Phase Transition," Nat. Commun. **6**, 1-5 (2015).

[32] D.G. Schlom, L.Q. Chen, X.Q. Pan, A. Schmehl, and M.A. Zurbuchen, "A Thin Film Approach to Engineering Functionality into Oxides," J. Am. Ceram. Soc. **91**, 2429–2454 (2008).

[33] A. Vassighi and S. Manoj, "Thermal and Power Management of Integrated Circuits," Springer Science and Business Media, New York, NY, U.S.A. 149-175 (2006).

[34] A. Vassilyeva, R. Eglitis, E. Kotomin, and A. Dauletbekova, "Ab Initio Calculations of the Atomic and Electronic Structure of MgF₂ (011) and (111) Surfaces," Cent. Eur. J. Phys. **9**, 515-518 (2011).

[35] B. Marinder, "Studies on Rutile-Type Phases in Mixed Transition Metal Dioxides. II.," Acta Chem. Scand. **16**, 293 (1962).